Journal of Maps

ISSN: (Print) (Online) Journal homepage: www.tandfonline.com/journals/tjom20

Glacial geomorphology of the northwest Laurentide Ice Sheet on the northern Interior Plains and western Canadian Shield, Canada

Helen E. Dulfer, Benjamin J. Stoker, Martin Margold & Chris R. Stokes

To cite this article: Helen E. Dulfer, Benjamin J. Stoker, Martin Margold & Chris R. Stokes (2023) Glacial geomorphology of the northwest Laurentide Ice Sheet on the northern Interior Plains and western Canadian Shield, Canada, Journal of Maps, 19:1, 2181714, DOI: 10.1080/17445647.2023.2181714

To link to this article: https://doi.org/10.1080/17445647.2023.2181714

JOURNAL OF MAPS
2023, VOL. 19, NO. 1, 2181714
https://doi.org/10.1080/17445647.2023.2181714

SCIENCE

OPEN ACCESS Check for updates

Glacial geomorphology of the northwest Laurentide Ice Sheet on the northern Interior Plains and western Canadian Shield, Canada

Helen E. Dulfer[a], Benjamin J. Stoker[a], Martin Margold[a] and Chris R. Stokes[b]

[a]Department of Physical Geography and Geoecology, Faculty of Science, Charles University, Prague, Czech Republic; [b]Department of Geography, Durham University, Durham, United Kingdom

ABSTRACT

The majority of the Northwest Territories of mainland Canada was covered by the Laurentide Ice Sheet during the Last Glacial Maximum. The increasing coverage of high resolution remotely sensed data provides new opportunities to map the glacial geomorphology and study the glacial history of this remote location. Here we present a comprehensive map of glacial landforms within the northern Interior Plains and adjacent areas of the Canadian Shield, comprising around 6% of the Laurentide Ice Sheet bed. Twelve landform types were mapped from the high resolution ArcticDEM: ice flow parallel lineations, subglacial ribs, crevasse-squeeze ridges, major and minor moraine crests, hummocky terrain complexes and ridges, shear margin moraines, major, minor and lateral and submarginal meltwater channels, esker ridges and complexes, glaciofluvial complexes, perched deltas, raised shorelines and aeolian dunes. Together, these landforms provide a record of the highly dynamic behaviour of the northwest sector of the Laurentide Ice Sheet.

ARTICLE HISTORY
Received 17 October 2022
Revised 9 February 2023
Accepted 11 February 2023

KEYWORDS
Laurentide Ice Sheet; glacial landforms; remote sensing; ArcticDEM; Northwest Territories; glacial history

1. Introduction

The Laurentide Ice Sheet (LIS) was the largest ephemeral Pleistocene ice sheet to grow and almost completely disappear during the last glacial cycle. At the Last Glacial Maximum (LGM) the LIS coalesced with the Cordilleran Ice Sheet (CIS) east of the Rocky Mountains, while the northwest sector of the LIS reached its all-time maximum extent along the eastern range fronts of the Mackenzie and Richardson mountains during the local LGM, around 22.1 cal ka BP (Figure 1; Kennedy et al., 2010). While the ice dynamics of this sector of the ice sheet and formation of glacial lakes along the retreating ice sheet margin have been interpreted on a broad scale (Lemmen et al., 1994; Dyke, 2004; Kleman & Glasser, 2007; Brown, 2012), a detailed understanding of the ice sheet configuration and the ice-drainage network, and how it changed through the ice advance and deglacial stages, remains incomplete (Margold et al., 2018).

The glacial geomorphology of the northwest sector of the LIS has been mapped by a number of researchers at a variety of scales. At a local to regional scale, much of the Northwest Territories is covered by detailed National Topographic System (NTS) surficial geological maps (see Figure 2 and references therein). At a broader scale, Brown et al. (2011) produced a glacial geomorphological map of the northwest sector of the LIS and Duk-Rodkin (2022) recently published a compilation map of the Mackenzie Mountains and foothills.

Prest et al. (1968) produced the Glacial Map of Canada, which was the first ice-sheet-wide map of glacial landforms. More recently, Shaw et al. (2010) and Kleman et al. (2010) both produced generalized ice flow maps of the entire North American Ice Sheet Complex, comprising the Cordilleran, Laurentide and Innuitian ice sheets at the LGM. However, large gaps remain in the spatial coverage of the surficial maps, while the broad scale map of Brown et al. (2011) lacks detail due to limited data resolution at the time of mapping. Thus, our knowledge of the glacial geomorphology of the northwest LIS can be augmented using newer high resolution digital elevation models (DEMs) now available for the region (Chandler et al., 2018; Stokes et al., 2015).

Recent work has focused on determining the timing of the deglaciation of the northwest sector of the LIS and subsequent opening of the ice-free corridor, which allowed for the exchange of flora and fauna between North America and unglaciated Beringia (Stoker et al., 2022; Clark et al., 2022; Reyes et al., 2022). However, our understanding of the glacial dynamics in this region remains poor, particularly with regards to the behaviour of the major ice streams (Margold et al., 2018) and the configuration of the ice

CONTACT Helen E. Dulfer dulferh@natur.cuni.cz Department of Physical Geography and Geoecology, Faculty of Science, Charles University, Albertov 6, 12800 Prague, Czech Republic

Supplemental map for this article can be accessed online at https://doi.org/10.1080/17445647.2023.2181714.

divides over time (Bednarski, 2008). Here, we use the high resolution ArcticDEM v3 mosaic (2 m resolution; Porter et al., 2018) to produce a detailed glacial landform map of the northwest sector of the LIS. The resulting glacial geomorphological map will underpin future investigations into the advance and retreat dynamics of this sector of the LIS.

2. Methods

2.1 Map area

The glacial landform map covers an area of approximately 900,000 km^2 and is bounded by the 60°N parallel to the south, the 110°W meridian to the east, the coastline of the Northwest Territories and Nunavut to the north (comprising the Beaufort Sea, Amundsen Gulf, Dolphin and Union Strait, and Coronation Gulf), and the edge of the Canadian Cordillera to the west (encompassing the Richardson and Mackenzie mountains; see the red outline in Figure 1). The map area is made up of two physiographic regions: (1) the Interior Plains on the western side, which contains the contemporary Mackenzie River Valley and Mackenzie Delta; and (2) the Canadian Shield on the eastern side, which is composed of Precambrian igneous and metamorphic rocks (Bostock, 2014; Slaymaker & Kovanen, 2017). The Precambrian shield boundary divides these two physiographic regions (Figure 1) and the eastern map boundary, along the 110°W meridian, was chosen so that the map covers the transition onto the shield area and subsequent change in subglacial bed composition. The map area covers approx. 6% of the LIS bed.

2.2. Data

Glacial geomorphological mapping was undertaken in ArcMap 10.6.1 using hill-shaded imagery derived from the ArcticDEM v3 mosaic with 2 m vertical resolution (Porter et al., 2018) and the Image Mosaic of Canada v1, which consists of Landsat bands 7 (red), 4 (green) and 2 (blue) with 30 m horizontal resolution (Government of Canada, 2013). Figure 2(b) shows the coverage of the ArcticDEM across our study area at the time of map production. All publicly available surficial geological maps were georeferenced in an ArcMap environment to assist with the identification of landforms (Figure 2(a)). These maps include the following: 1:50,000 scale surficial geological maps (Bednarski, 2002; Bednarski, 2003a, 2003b, 2003c, 2003d, 2003e, 2003f, 2003g, 2003h, 2003i, 2003j, 2003k, 2003l, 2003m, 2003n, 2003o), p. 1:100,000 scale surficial geological maps (Duk-Rodkin, 2009a, 2009b, 2010a, 2010b, 2011a, 2011b, 2011c, 2011d; Duk-Rodkin & Huntley, 2018; Smith et al., 2021; Hagedorn et al., 2022); 1:125,000 scale surficial geological maps (Klassen, 1971; Rutter et al., 1980; St-Onge, 1988; Olthof et al., 2014; Geological Survey of Canada, 2014a, 2014c, 2015, 2016c, 2016d, 2017b, 2017c, 2018a, 2018b, 2019a, 2019b, 2019c, 2019d, 2022b, 2022c; Ednie et al., 2014; Kerr, 2014, 2018, 2022a, 2022b, 2022c, 2022d, 2022e; Kerr et al., 2014, 2016, 2017a, 2017b; Kerr & O'Neil, 2017, 2018a, 2018b, 2019a, 2019b, 2019c, 2020, 2021; Morse et al., 2016; Stevens et al., 2017; Paulen & Smith, 2022); 1:250,000 scale surficial geological maps (Duk-Rodkin, 1989, 1992; Duk-Rodkin & Hughes, 1992a, 1992b, 1992c, 1992d, 1992e, 1992f, 1993a, 1993b; Duk-Rodkin & Couch, 2004; Veillette et al., 2013a, 2013b; Geological Survey of Canada, 2014b, 2016a, 2016b, 2017a, 2022a), 1:500,000 scale surficial geological maps (Rutter et al., 1993) (see Figure 2(a) for map locations). In addition, district-scale geomorphological maps (Craig, 1960, 1965; Rampton, 1988), geomorphological and sedimentological studies (e.g. Huntley et al., 2008; Evans et al., 2021), a compilation map of the Mackenzie mountains and foothills at the 1:1,000,000 scale by Duk-Rodkin (2022) and the glacial landform map of Brown et al. (2011) were also consulted.

2.3 Landform mapping

The study area was divided in half along the 65°N parallel and the two halves were mapped independently by the first two authors. To ensure consistency, a trial area was initially chosen for both researchers to map simultaneously. Their resulting maps were then compared by all team members and the glacial landform categories were defined using both polygon and polyline shapefiles. Following best-practice (Chandler et al., 2018), both researchers then used a repeat-pass method to identify each landform in their respective study areas using a variety of scales between 1:50,000 and 1:100,000. To ensure further consistency, once mapping was completed, the two researchers switched map areas and checked each other's mapped landforms. The resulting landform shapefiles were then combined into a single map. Each landform has been identified from the imagery based on its morphology, spatial arrangement and association with other landforms as outlined below. The map does not include glacial landforms produced by local montane ice masses in the Mackenzie Mountains.

2.3.1 Ice flow parallel lineations

Ice flow parallel lineations include drumlins, flutes, mega-scale glacial lineations, streamlined bedrock and crag-and-tails (see Figure 3 for examples). These landforms represent a variety of depositional and erosional ridges formed subglacially that are elongate parallel to palaeo-ice flow (Boulton & Clark, 1990a, 1990b; Clark, 1993, 1999; King et al.,

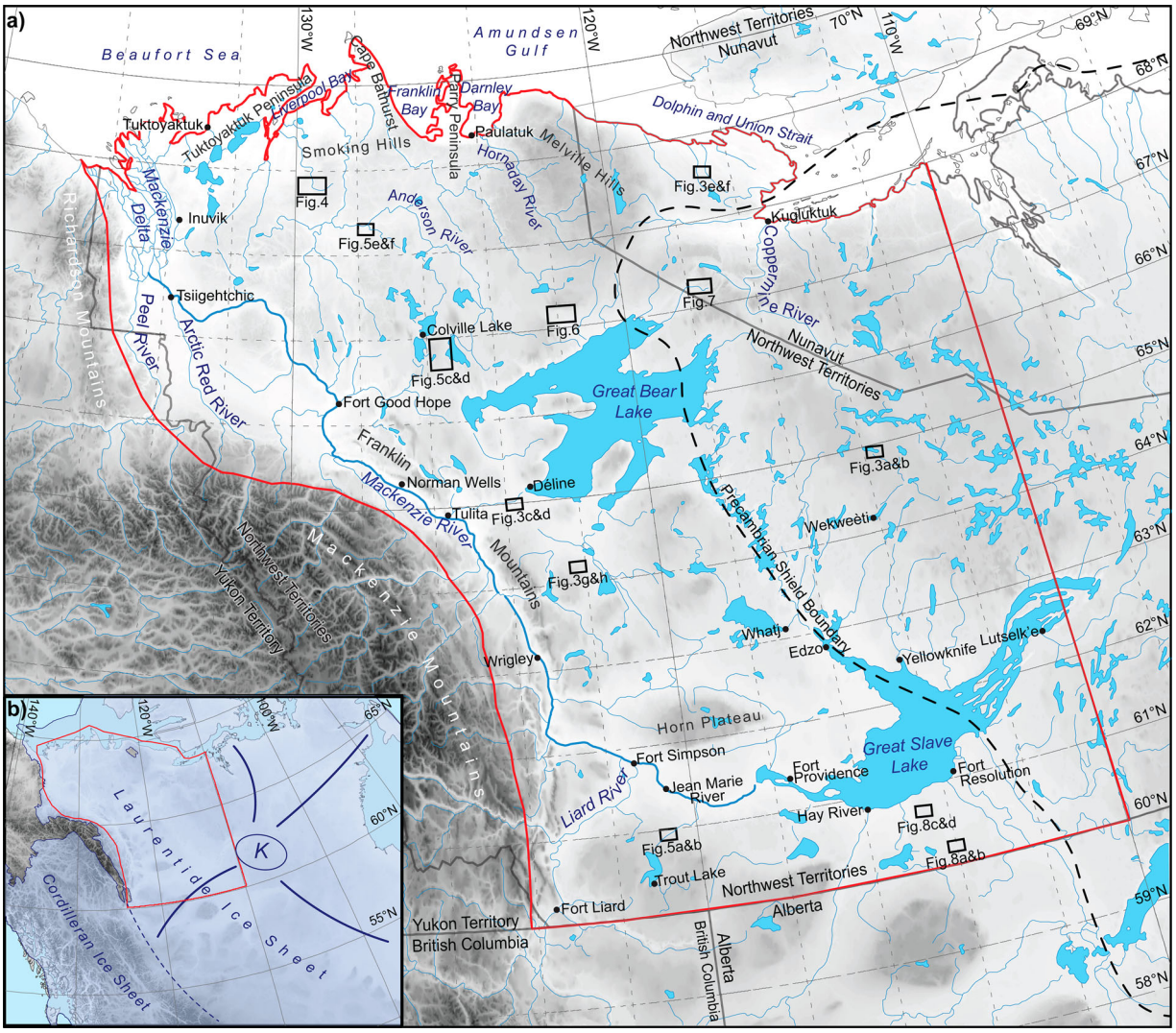

Figure 1. (a) Map showing the extent of the glacial geomorphological map produced in this study (red outline). Elevation data from the 30 Arc-Second DEM of North America (EROS, 2010). Major physiographic features and place names are shown (Natural Resources Canada, 2012). The dashed black line delineates the two major physiographic regions: the Interior Plains to the west and the Canadian Shield to the east. The location of Figures 3–8 are shown by the black boxes. (b) Inset map showing northwestern sector of the North American Ice Sheet Complex at 22.1 cal ka BP drawn from Dalton et al. (2020) with the approximate position of the ice divides and the Keewatin ice dome (K) drawn in dark blue and the coalescence between the LIS and CIS shown by the blue dashed line (Margold et al., 2018).

2009). Additionally, this category includes lineations that were identified by a distinct colour change in the Image Mosaic of Canada v1, and which may be related to a subtle topographic expression (Figure 4). Each landform crest was drawn as a single line and the ice flow direction was drawn with an arrow where the stoss and lee side of the lineation could be identified. Ice flow parallel lineations usually occur in fields or swarms made up of hundreds of lineations with similar morphology, spacing and orientation.

2.3.2 Subglacial ribs

Subglacial ribs, also termed ribbed moraine, traction ribs or Rogen moraine, consist of large ridges of sediment that are formed subglacially and usually occur in swarms (Aylsworth & Shilts, 1989; Lundqvist, 1989; Hättestrand & Kleman, 1999; Dunlop & Clark, 2006). Individual ribs may be curved and may have an asymmetric cross-profile (Figure 3(e, f)). Subglacial ribs often occur in fields made up of multiple ribs, and although the morphology and size of subglacial ribs is highly variable (Dunlop & Clark, 2006; Stokes et al., 2016), ribs belonging to the same field often have a regular shape.

2.3.3 Crevasse-squeeze ridges

Crevasse-squeeze ridges are linear, curvilinear or inverted v-shaped ridges of glacial sediment (Figure 5(a, b)) (Boulton et al., 1996; Norris et al., 2017). Crevasse-squeeze ridges often form geometrical ridge networks, with straight or slightly arcuate ridges intersecting at right angles (Evans et al., 2016). Crevasse-squeeze ridges can cross-cut each other.

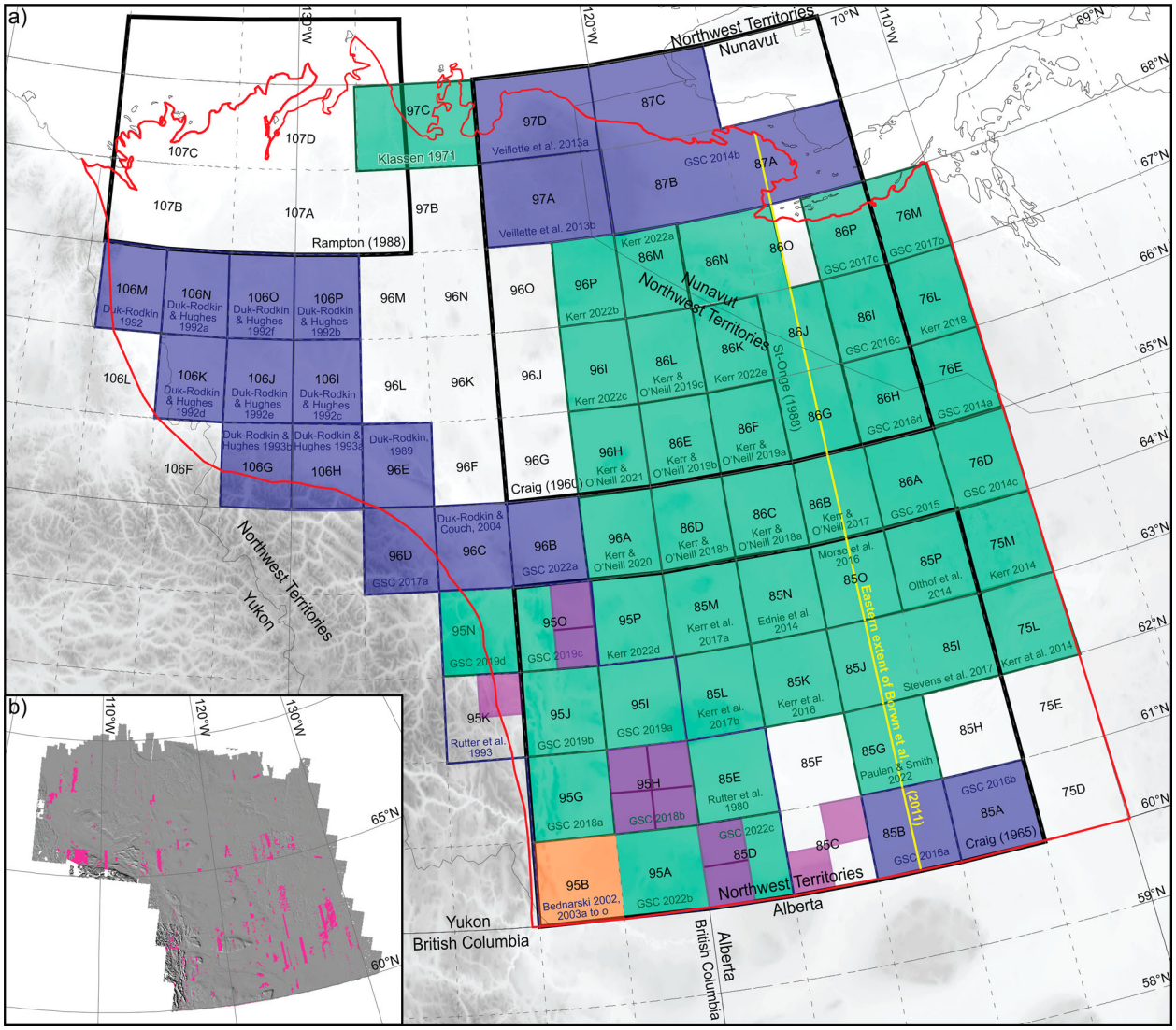

Figure 2. (a) Map showing the extent of the glacial geomorphological map produced in this study (red outline) and previously published maps. The national topographic tiles that intersect the mapped area are labelled. The coverage of 1:250,000 (blue shading), 1:125,000 (green shading), 1:100,000 (purple shading) and 1:50,000 (orange shading) surficial geology maps from the Geological Survey of Canada are shown. The 1:100,000 scale maps are from Duk-Rodkin (2009a,2009b, 2010a,2010b,2011a,2011b,2011c,2011d), Duk-Rodkin and Huntley (2018), Smith et al. (2021) and Hagedorn et al. (2022). The black boxes correspond to broad-scale glacial geomorphological maps. The yellow line shows the eastern extent of the glacial geomorphological map of Brown et al. (2011). (b) Map showing the coverage of the ArcticDEM. Hillshade imagery derived from the ArcticDEM is shown in grey (Porter et al., 2018) and the pink colour highlights the voids in the current coverage of the DEM.

2.3.4 Moraines

Terminal moraines occur as broadly linear, straight or arcuate-shaped ridges that form by the deposition or deformation of glaciogenic sediment at the margins of active glaciers (Figure 5(c, d)) (Benn & Evans, 2010). Moraines can exhibit both sharp and broad ridge crests. Where the moraine is >200 m wide it was mapped as a polygon (moraine crest major) and where it is <200 m wide it was mapped as a polyline (moraine crest minor). Where the identification of the moraine is more speculative, it was mapped as an uncertain moraine.

2.3.5 Hummocky terrain

Hummocky terrain is an irregular undulating surface consisting of mounds of sediment alternating with depressions (Figure 6) (Brown et al., 2011; Stroeven et al., 2013; Lindholm & Heyman, 2016). Hummocky terrain displays a diverse range of morphologies, which can appear chaotic and irregular. Where distinct linear and curvilinear ridges occur within hummocky terrain they were marked with a polyline.

2.3.6 Shear margin moraines

Shear margin moraines consist of long (10–30 km), broad ridges of sediment located at the edge of a field of highly attenuated streamlined landforms (Figure 6) (Dyke & Morris, 1988; Stokes & Clark, 2002). Shear margin moraines were mapped as a polyline along the crest or center of the ridge.

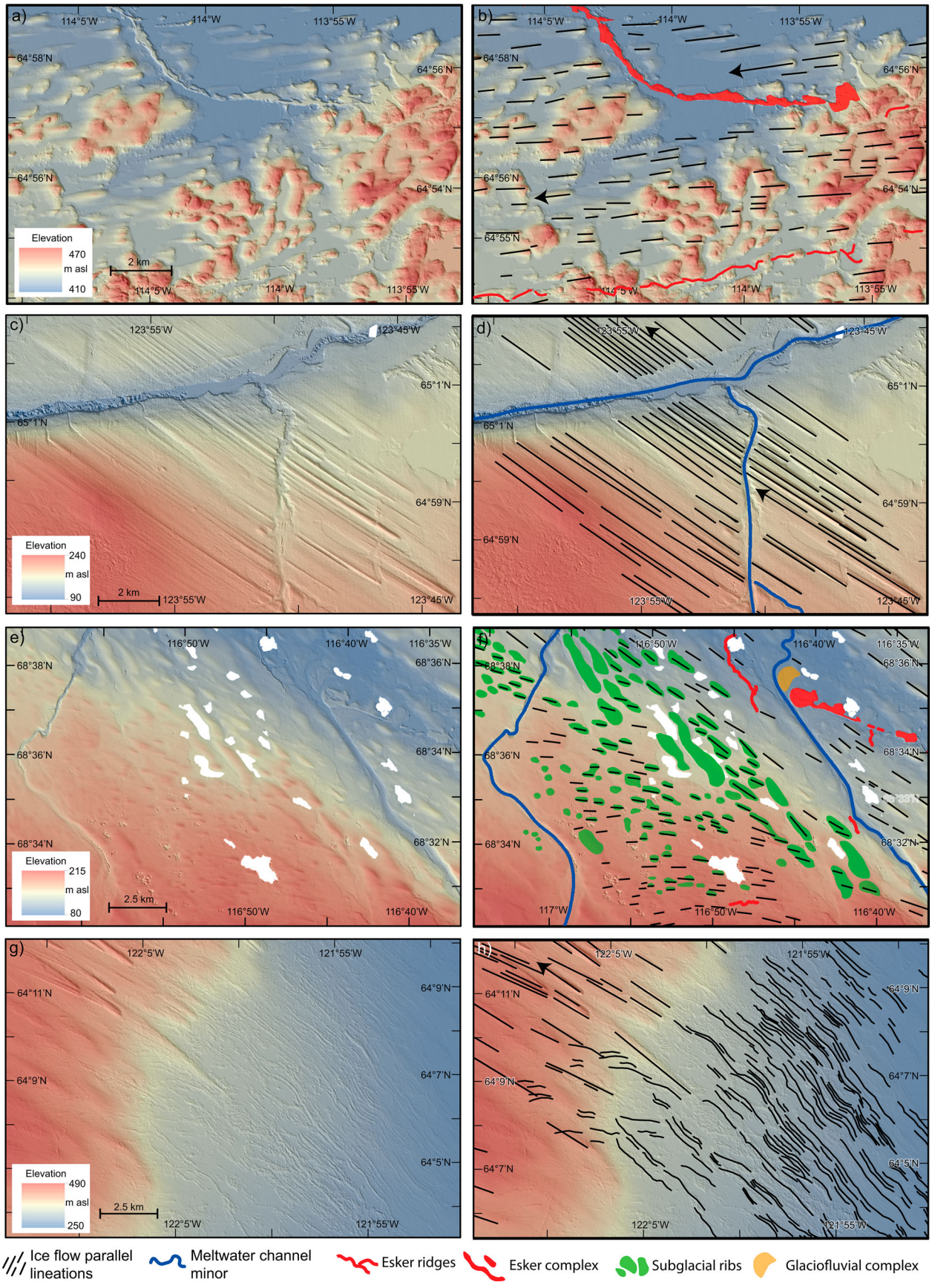

Figure 3. Examples of different types of ice flow parallel lineations. (a) ArcticDEM-derived hillshade imagery and (b) geomorphological mapping of crag-and-tails and streamlined bedrock on the Canadian Shield. The stoss and lee side of the crag-and-tail can be inferred, giving the ice flow direction. Additionally, linear depositional ridges and flat-top accumulations of sediments are interpreted as eskers. (c) ArcticDEM-derived hillshade imagery and (d) geomorphological mapping of drumlins and mega-scale glacial lineations. (e) ArcticDEM-derived hillshade imagery and (f) geomorphological mapping of ice flow parallel lineations with a variable direction superimposed on subglacial ribs. Meltwater channels, eskers and glaciofluvial complex are also mapped. (g) ArcticDEM-derived hillshade imagery and (h) geomorphological mapping of wavy groove-plough lineations at lower elevations and drumlins at higher elevations. Note that the ridge crest between the groove-plough has been digitized. The location of these figures is shown in Figure 1. The incident light azimuth is 315°, the incident light angle is 35° and the vertical exaggeration is 2 across all DEM images.

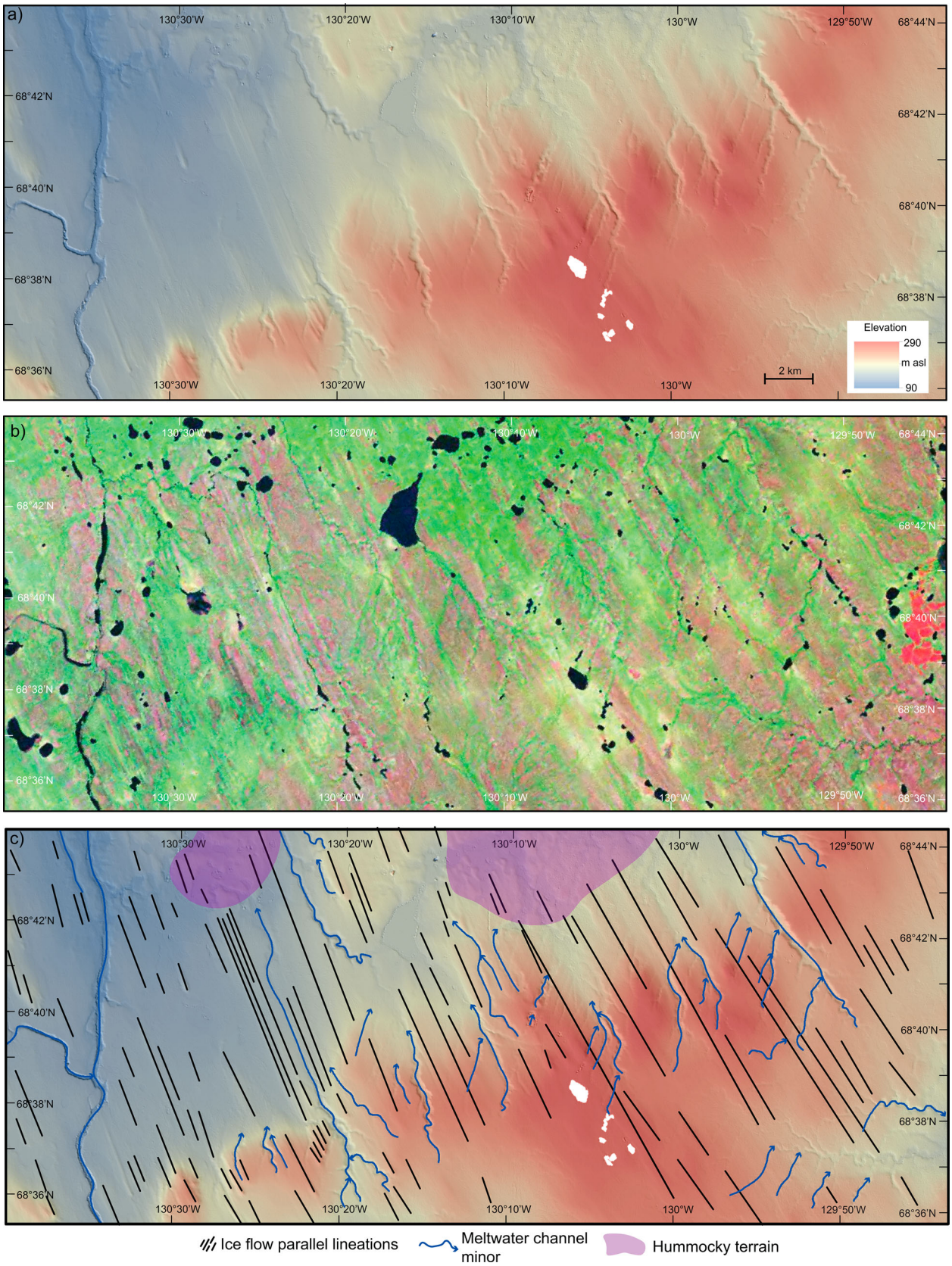

Figure 4. Example of ice flow parallel lineations identified within the Image Mosaic of Canada v1. (a) ArcticDEM-derived hillshade imagery (incident light azimuth: 315° and angle: 35°; vertical exaggeration is 2) (b) Landsat satellite imagery with Landsat bands 7 (red), 4 (green) and 2 (blue) (Image Mosaic of Canada v1; Government of Canada, 2013) and (c) geomorphological mapping. The location of this figure is shown in Figure 1.

2.3.7 Meltwater channels

Meltwater channels form in three main locations in relation to an ice mass: lateral and submarginal meltwater channels form by water flowing along ice margins; subglacial meltwater channels are formed by channelized flow at the bed of the ice sheet; and proglacial

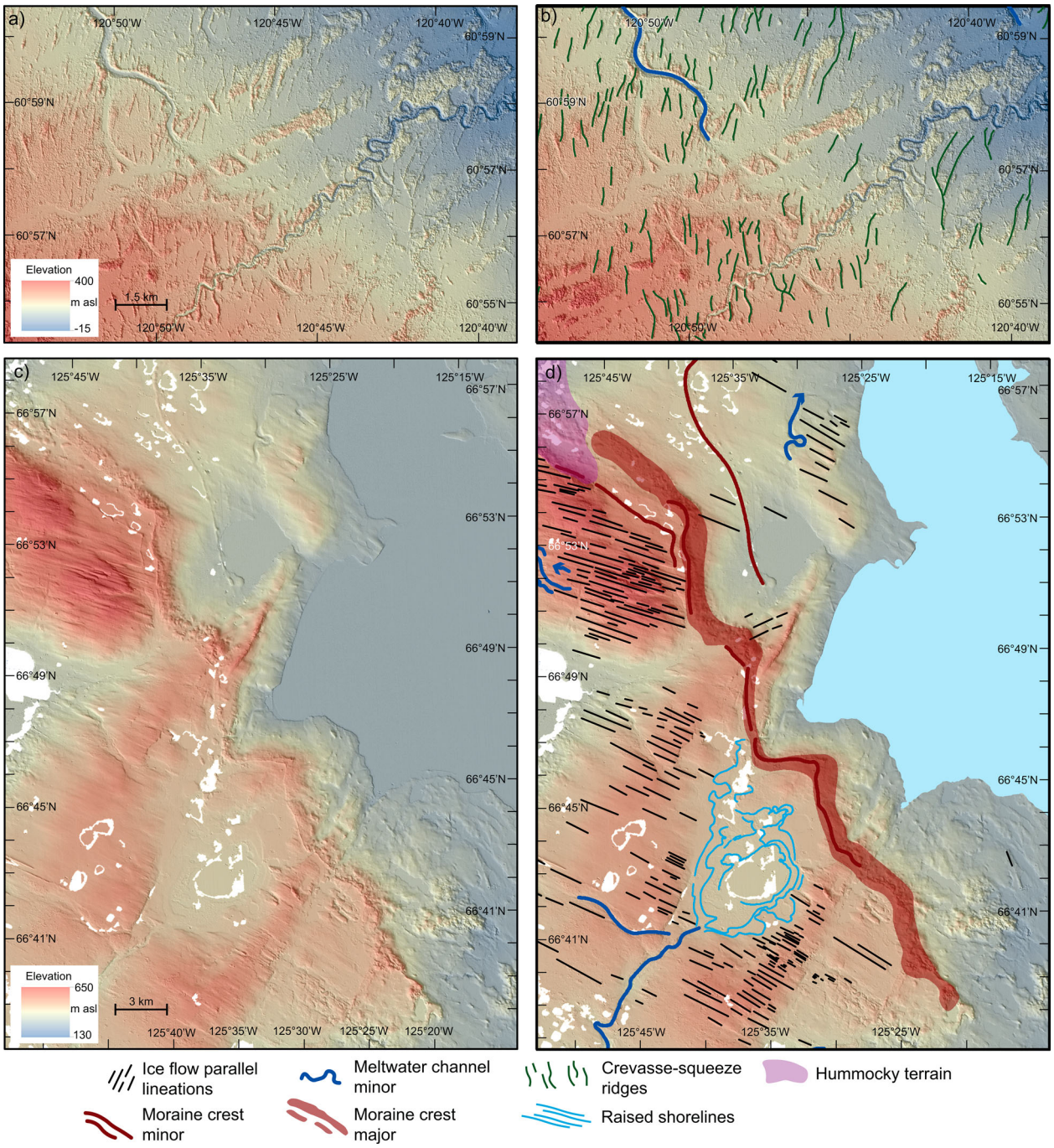

Figure 5. (a) ArcticDEM-derived hillshade imagery and (b) geomorphological mapping of crevasse-squeeze ridges. (c) ArcticDEM-derived hillshade imagery and (d) geomorphological mapping of major and minor moraine crests. Ice flow parallel lineations, meltwater channels and raised shorelines are also mapped. The location of these figures is shown in Figure 1. The incident light azimuth is 315°, the incident light angle is 35° and the vertical exaggeration is 2 across all DEM images.

meltwater channels are formed by water draining away from the ice sheet terminus (Mannerfelt, 1949; Greenwood et al., 2007, 2016; Margold et al., 2011). Here, we map subglacial and proglacial meltwater channels as one meltwater channel category as they can be difficult to distinguish based on geomorphology alone and, in many cases, the channels may transport different sources of meltwater at different stages of the ice sheet evolution. Thus, these meltwater channels have a wide range of sizes, morphologies and sinuosities, and contain bifurcating and anastomosing channels. Where the meltwater channel is <1 km wide we draw a polyline in the center of the incised topography and where it is >1 km wide we draw a polygon encompassing the entire channel.

Lateral and submarginal meltwater channels are distinguished in our map as a regular series of parallel or subparallel channels that dip in the same direction and have low to medium sinuosity (Figure 6) (Greenwood et al., 2007, 2016). Lateral and submarginal meltwater channels often occur as a sequence of channels perched on the valley sides and sub-parallel to local contours. Channel networks are uncommonly observed and they may terminate in downslope chutes. Lateral and submarginal meltwater channels

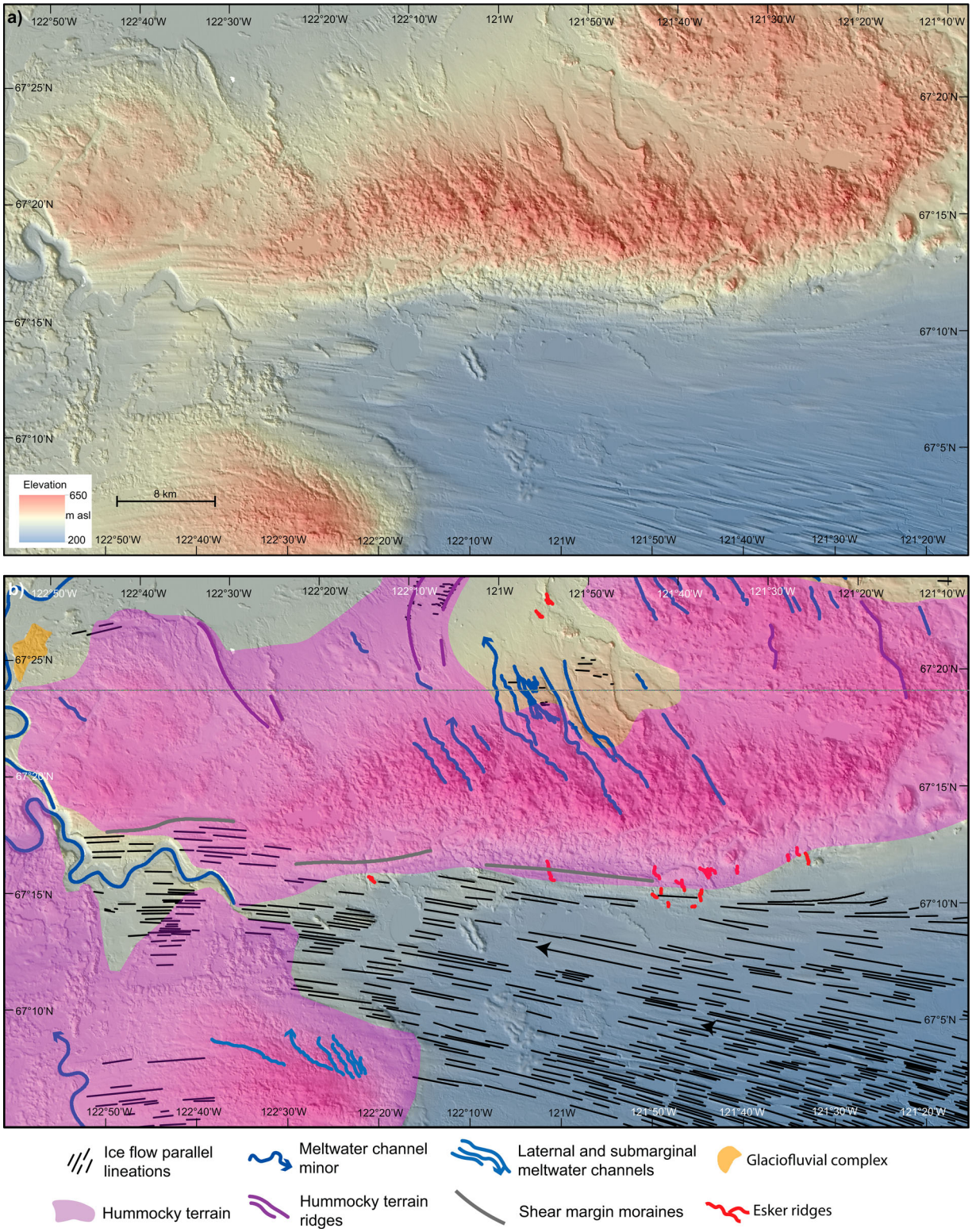

Figure 6. (a) ArcticDEM-derived hillshade imagery (incident light azimuth: 315° and angle: 35°; vertical exaggeration is 2) and (b) geomorphological mapping. The irregular undulating surfaces at high elevations is mapped as hummocky terrain (purple polygon) and shear margin moraines mark the transition between the corridor of highly attenuated bedforms and the hummocky terrain. The two different categories of meltwater channels and eskers are also mapped. The location of this figure is shown in Figure 1.

are drawn as a polyline in the center of the incised topography.

2.3.8 Eskers

Eskers are sinuous depositional ridges of glaciofluvial sand and gravel (Shreve, 1985; Hebrand & Åmark, 1989; Storrar et al., 2014). Individual esker ridges often align to form networks up to 200 km long, but the morphology along the network may vary from continuous esker ridges to large esker complexes or deltas (Figure 7) (Margold et al., 2011; Storrar et al., 2020). Individual esker ridges were mapped as a

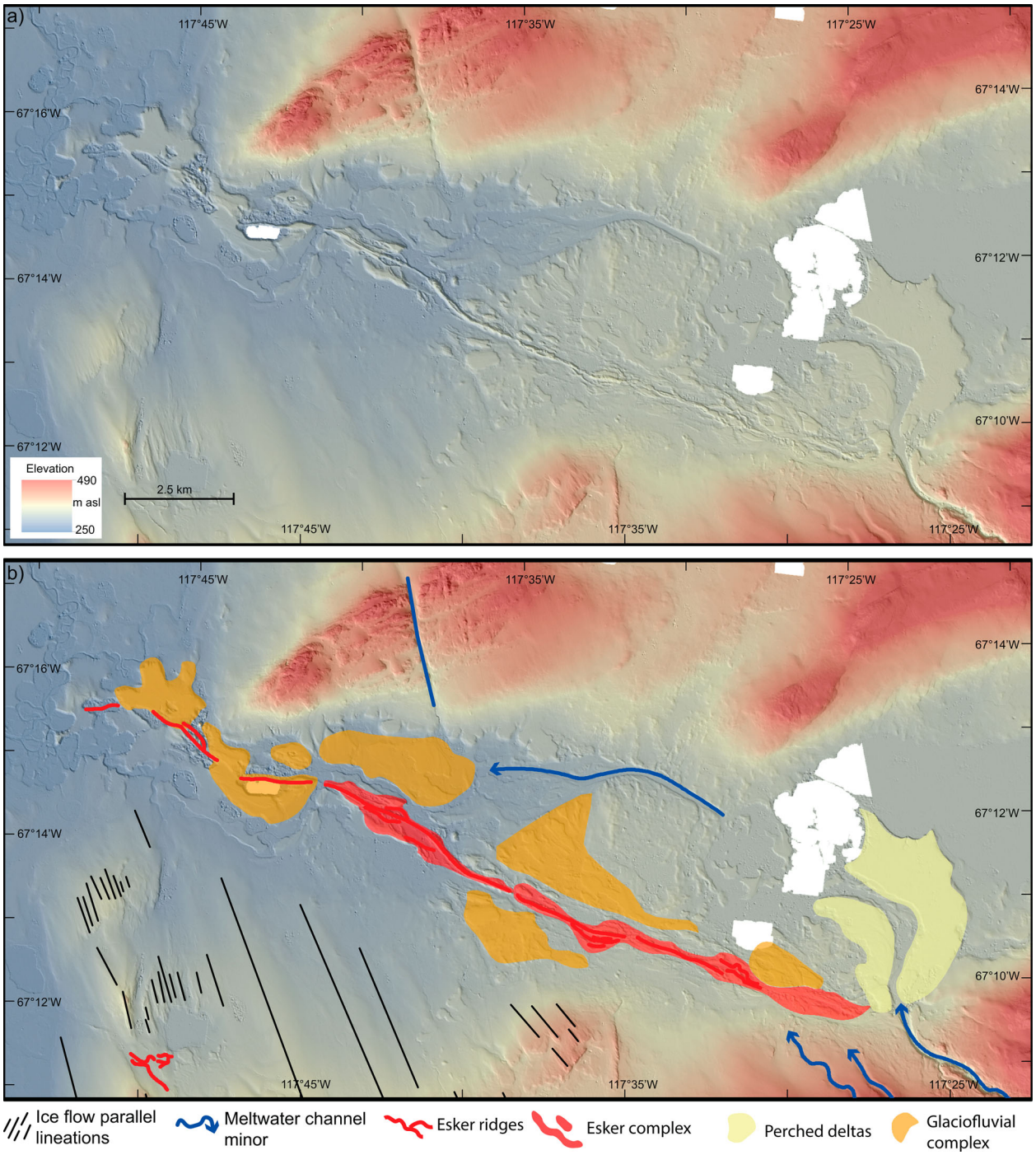

Figure 7. Example of the glacial meltwater landforms. (a) ArcticDEM-derived hillshade imagery (incident light azimuth: 315° and angle: 35°; vertical exaggeration is 2) and (b) geomorphological mapping of flat topped deltas, esker ridges and complexes and glaciofluvial complexes. Meltwater channels and ice flow parallel lineations were also mapped. The location of this figure is shown in Figure 1.

polyline along the ridge crest and eskers with a complex morphology were mapped as a polygon around the esker complex.

2.3.9 Glaciofluvial complex

Glaciofluvial complexes are deposits of glaciofluvial sand and gravel that can have a wide variety of morphologies, including flat topped, channelized, pitted or ridged deposits (see Figure 7). Glaciofluvial complexes also form in a wide variety of environments, including within or at the terminus of meltwater channels, proximal to or associated with eskers, or perched on valley walls (known as kame terraces).

2.3.10 Perched deltas

Deltas form when sediment that is transported by a river or stream is discharged into a body of water (e.g. a lake). Deltas can be identified by flat top surfaces and steeply dipping frontal beds (Figure 7). Perched deltas are deposited into transient ice-dammed lakes that form when the natural water drainage path is blocked by a retreating ice margin

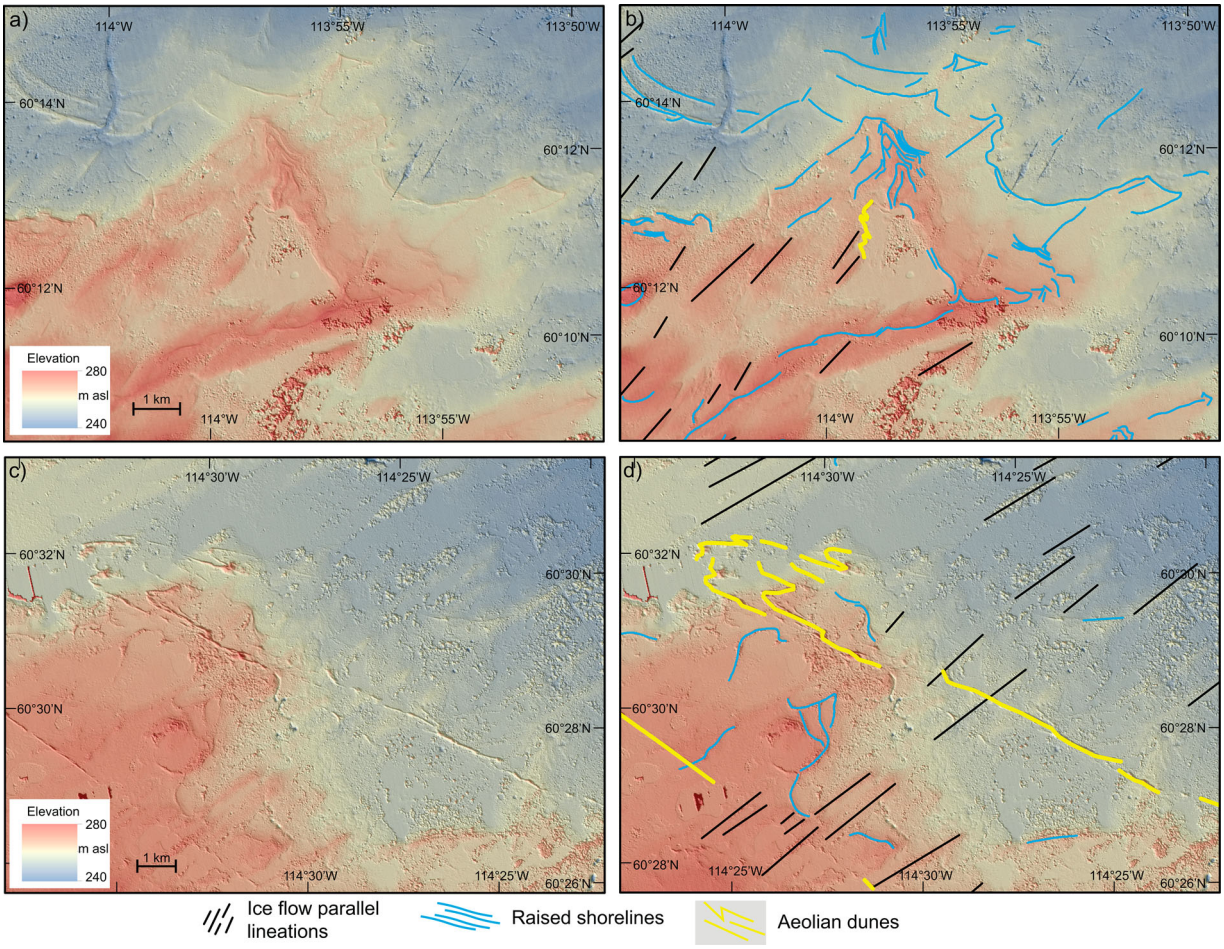

Figure 8. Examples of raised shorelines and aeolian dunes. (a), (c) ArcticDEM-derived hillshade imagery (incident light azimuth: 315° and angle: 35°; vertical exaggeration is 2) and (b), (d) geomorphological mapping. The raised shorelines consist of beach ridges deposited parallel to the topography. The aeolian dune ridges are straight ridges that sometimes form a zig-zag pattern and can cross-cut the glacial landforms. The location of this figure is shown in Figure 1.

(Mannerfelt, 1949; Stroeven et al., 2016; Dulfer & Margold, 2021). These deltas remain perched on the valley slopes once the glacial lake drains.

2.3.11 Raised shorelines

Raised shorelines are small (<200 m wide) continuous linear ridges or benches that form parallel to topography but may be tilted over time due to differential glacial isostatic uplift (Figure 8). Raised shorelines usually occur as a series and may stretch for tens of kilometers. Raised shorelines form by the erosion or deposition of sediment along a former shoreline, forming a wave-cut cliff or beach ridge.

2.3.12 Aeolian dunes

Longitudinal and parabolic aeolian dunes are distinctive ridges of aeolian sediment that range in size from a few hundred meters to tens of kilometers (Figure 8). Aeolian dunes often have sharp crests and they can occur as a field of dunes or as single longitudinal landforms. Fields of aeolian dunes have been previously identified across the once glaciated regions of Canada (Koster, 1988; Wolfe et al., 2004; Bateman & Murton, 2006; Norris et al., 2017). We choose to include aeolian dunes as the only non-glacial landform in our map because, in northern Canada, they are relict features that likely formed by the windblown re-deposition of glaciofluvial and glaciolacustrine sediment within cold environments directly following deglaciation. The dune crest is digitised as a polyline.

2.4 Accuracy and completeness

Our large study area (~900,000 km^2) is covered by high resolution remotely sensed data (2 m resolution) and, therefore, it is not possible to capture every glacial landform (for example, every ice flow parallel lineation within a swarm of lineations). However, we believe our repeat pass mapping method using a variety of scales has allowed us to map the representative distribution of landforms across the entire study area. We acknowledge that some of the mapped glacial landforms may be misinterpreted. For example, in some cases eskers can be difficult to distinguish from moraines, dykes and dunes, but, they are usually differentiated based on their high sinuosity and association with other meltwater landforms. Similarly, small recessional moraines and crevasse-squeeze ridges can be difficult to differentiate. We acknowledge that our

record of the smaller glacial landforms, such as crevasse-squeeze ridges, may be incomplete as their size is often at or below the resolution of our mapping data. However, our map can be used in combination with existing surficial geological maps that may capture these smaller glacial landforms, as they were often mapped with stereo pairs of aerial photographs.

3. Results

3.1 Ice flow parallel lineations

In total, 76,630 ice flow parallel lineations were mapped throughout the study area. In general, our ice flow parallel lineations match, but add considerable detail to, the generalized flow maps of both Kleman et al. (2010) and Shaw et al. (2010) and the glacial geomorphological map of Brown et al. (2011). The mapped ice flow parallel lineations usually occur in discrete swarms of lineations with similar size, spacing and orientation, which can collectively form convergent and divergent patterns. Cross-cutting lineations occur in a number of locations and ice flow parallel lineations can be superimposed on subglacial ribs (Figure 3(e, f)), indicating that ice flow direction varied over time.

The mapped lineations range in size from tens of meters to 30 km in length, with the longest of these lineations having the dimensions of mega-scale glacial lineations (MSGLs), which typically have elongation ratios >10:1 (Stokes & Clark, 1999) and range in length from a few thousand metres to tens of kilometres (Spagnolo et al., 2014) (Figure 3(c, d)). A wide variety of ice flow parallel lineations occur across the map area that may represent varying subglacial depositional and erosional environments, including drumlins, flutes, crag-and-tails (Figure 3(a, b)), and MSGLs (Figure 3(g, h)).

3.2 Subglacial ribs

In total, 2396 subglacial ribs were mapped across the study area. The subglacial ribs vary in length (transverse to flow) from 0.1 km to 15 km and they have a variety of shapes. However, ribs belonging to the same swarm usually have a regular size and morphology. Subglacial ribs are located at a variety of elevations, occurring on the valley floors as well as on the high elevation plateaus. Ice flow parallel lineations are often superimposed on subglacial ribs and the varying orientation of the ribs and lineations can indicate the ice flow direction has varied over time (Figure 3(e, f)) (Ely et al., 2016).

3.3 Crevasse-squeeze ridges

In total, 2110 crevasse-squeeze ridges have been mapped. They generally occur in fields as short (<3 km), narrow, straight or wavy ridges of sediment with irregular spacing. They are sometimes superimposed on other subglacial bedforms, such as drumlins, and they are often orientated perpendicular to the surrounding ice flow parallel lineations.

3.4 Moraines

A total of 44 major moraine crests (polygon) and 768 minor moraine crests (polyline) have been mapped across the study area. Additionally, 210 uncertain moraine crests have been mapped (polyline). Multiple moraine crests can be linked together to form a moraine complex that is up to 70 km long and 2 km wide. The geometry of moraine crests is influenced by the topography and they are often aligned with other ice marginal glacial landforms (Figure 5(c, d)). Moraine crests consist of both terminal and lateral moraines and they sometimes occur as a series of recessional moraines.

3.5 Hummocky terrain

Within our map, the majority of hummocky terrain is located in the northwest (Main Map) where large areas of hummocky terrain up to 250 km wide have been mapped. In the south, hummocky terrain is mapped on many of the high elevation plateaus of the Interior Plains, while it has a limited distribution the Canadian Shield to the east, where it is mapped north of Lac de Gras. Within the hummocky terrain polygons, 330 ridges have been mapped along their crestline and these ridges display a wide variety of morphologies from broad ridges of hummocky sediment up to 5 km wide to narrow, sharp-crested ridges (<200 m wide). We note that these ridges are sometimes mapped as moraine crests within the surficial maps from the Geological Survey of Canada (e.g. Duk-Rodkin & Hughes, 1992b,1992f).

3.6 Shear margin moraines

Seven shear margin moraines have been mapped in the study area and they range in length from 5.5 km to 13 km. All mapped shear margin moraines occur at the edge of hummocky terrain and mark the transition between attenuated bedforms and hummocky terrain (Figure 6). The mapped shear margin moraines occur at the edge of previously mapped paleo-ice streams (Margold et al., 2015a, 2015b).

3.7 Meltwater channels

In total, 42 major meltwater channels (>1 km wide), 4266 minor meltwater channels (<1 km wide) and 1338 lateral and submarginal meltwater channels have been mapped across the study area. These channels display a wide range of morphologies, occur across all elevations, and can be several hundred

kilometers long. The mapped meltwater channels are evenly distributed across the study area, but the majority of the major meltwater channels are located in the northern section.

3.8 Eskers

In total, 290 esker complexes and 9543 esker ridges have been mapped. While the eskers display a full range of orientations, a large majority of mapped eskers have an east–west orientation. Esker ridges have been mapped throughout the study area, however, more than half of these ridges (~5200) occur on the Canadian Shield on the eastern side. Here, esker ridges often link together to form an esker network several hundred kilometers in length.

3.9 Glaciofluvial complex

In total, 218 glaciofluvial accumulations have been mapped within the study area. They range in size from a few hundred meters to 20 km in length and are up to 1 km wide. They occur throughout the study area and are often associated with other deglacial meltwater landforms, such as eskers and perched deltas (Figure 7).

3.10 Perched deltas

In total, 57 perched deltas have been mapped across the study area. They range in size from a few hundred meters up to 5 km in length and width and sometimes occur as a series of successive deltas at different elevations. Perched deltas occur throughout the study area.

3.11 Raised shorelines

In total, 16,401 raised shorelines have been mapped. They usually occur as a series of parallel ridges or notched flat surfaces that range in size from a few hundred meters to 30 km in length and they can be superimposed on other glacial landforms, such as drumlins and eskers. Raised glaciomarine shorelines have been mapped along the coastline of Nunavut and the Northwest Territories where they record the relative fall in sea level since the LGM. Inland, raised glaciolacustrine shorelines have been extensively mapped through the center of the study area and these mark the former extent of glacial lakes in the region, including glacial lakes McConnell and Mackenzie (Lemmen et al., 1994; Dyke, 2004).

3.12 Aeolian dunes

In total, 496 aeolian dunes have been mapped and they range in size from a few hundred meters to 22 km in length. The mapped aeolian dunes have a wide variety of morphologies, but usually occur as a field of dunes that have a regular size and morphology (Figure 8). Within our map area, aeolian dunes are mapped in small fields across the Interior Plains but we could not detect any on the Canadian Shield.

4. Conclusions and implications

The accompanying Main Map provides a detailed record of the glacial landforms of the northwest sector of the LIS. Supplementary figures S1 to S3 show that our map considerably adds to the landform record described in the existing literature (see Figure 2 and references therein) because it contains a high level of detail, similar to the landform content of many of the surficial geological maps produced by the Geological Survey of Canada, but covers a much greater area (more than 82 NTS map tiles), allowing the mapped surficial glacial geomorphology to be interpreted on an ice-sheet-wide scale. Furthermore, this is the first broad-scale map of this region for many of our landform categories, including crevasse-squeeze ridges, shear margin moraines, lateral and submarginal meltwater channels, glaciofluvial complexes, perched deltas, raised shorelines and aeolian dunes, which adds considerable detail when compared with the broad-scale glacial landform map of Brown et al. (2011) (see supplementary figures) and the Glacial Map of Canada (Prest et al., 1968). Thus, this glacial geomorphological map provides additional information that augments our understanding of the complex history of the northwest sector of the LIS during the last deglaciation. Using the glacial inversion method, which is the standard approach employed in empirical palaeo-ice sheet reconstructions (e.g. Kleman & Borgström, 1996; Kleman et al., 1997, 2006; Dulfer et al., 2022), the map data can now be used to determine the configuration of the northwest sector of the LIS over time, and in particular, understand the dynamics of this sector of the ice sheet during the last deglaciation.

Software

The hillshade surfaces were produced from the ArcticDEM data within ESRI ArcMAP 10.6.1. On-screen digitizing of landforms was also undertaken in ArcMAP 10.6.1 in the ESRI shapefile format. Once mapping was complete, a pdf map was exported from ArcMAP 10.6.1 and the final map was created in Adobe Illustrator 2022.

Availability of data

The ESRI shapefiles produced for each landform category are supplied with this paper.

Open Scholarship

This article has earned the Center for Open Science badge for Open Data. The data are openly accessible at https://doi.org/10.6084/m9.figshare.22040780.v1.

Acknowledgements

We acknowledge the First Nation people of the Northwest Territories and Nunavut, Canada, as the traditional owners of the land. The authors would like to thank Rod Smith for checking our inventory of surficial geological maps and helpful discussions about mapping in the Northwest Territories. Chris Clark, Colm O'Cofaigh and David Evans are thanked for participating in a workshop focused on the northwest sector of the LIS held at Durham University in December 2021. Heike Apps, Jeremy Ely and Roger Paulen are thanked for their constructive reviews of the map and manuscript.

Disclosure statement

No potential conflict of interest was reported by the author(s).

Funding

HED and BJS acknowledge support by the project Grant Schemes at Charles University (reg. no. CZ.02.2.69/0.0/0.0/19_073/0016935; START/SCI/055). HED and BJS were fully supported by the START research project during all stages of this work.

References

Aylsworth, J. M., & Shilts, W. W. (1989). Bedforms of the keewatin Ice sheet, Canada. *Sedimentary Geology*, *62* (2-4), 407–428. https://doi.org/10.1016/0037-0738(89)90129-2

Bateman, M. D., & Murton, J. B. (2006). The chronostratigraphy of late pleistocene glacial and periglacial aeolian activity in the tuktoyaktuk coastlands, NWT, Canada. *Quaternary Science Reviews*, *25*(19-20), 2552–2568. https://doi.org/10.1016/j.quascirev.2005.07.023

Bednarski, J. M. (2002). *Surficial geology, Fisherman Lake, Northwest Territories – Yukon Territory.* Geological Survey of Canada, Open File 4360, scale 1:50,000. https://doi.org/10.4095/213653.

Bednarski, J. M. (2003a). *Surficial geology, Arrowhead Lake, Northwest Territories.* Geological Survey of Canada, Open File 1775, scale 1:50,000. https://doi.org/10.4095/214449.

Bednarski, J. M. (2003b). Surficial geology, Arrowhead River, Northwest Territories. Geological Survey of Canada, Open File 4483, scale 1:50,000. https://doi.org/10.4095/214618.

Bednarski, J. M. (2003c). Surficial geology, Betalamea Lake, Northwest Territories – Yukon Territory. Geological Survey of Canada, Open File 4502, scale 1:50,000. https://doi.org/10.4095/214790.

Bednarski, J. M. (2003d). Surficial geology, Celibeta Lake, Northwest Territories – British Columbia. Geological Survey of Canada, Open File 1754, scale 1:50,000. https://doi.org/10.4095/214417.

Bednarski, J. M. (2003e). Surficial geology, Denedothada Creek, Northwest Territories. Geological Survey of Canada, Open File 4480, scale 1:50,000. https://doi.org/10.4095/214603.

Bednarski, J. M. (2003f). Surficial geology, Emile Lake, Northwest Territories. Geological Survey of Canada, Open File 4477, scale 1:50,000. https://doi.org/10.4095/214560.

Bednarski, J. M. (2003g). Surficial geology, Fort Liard, Northwest Territories – British Columbia. Geological Survey of Canada, Open File 1760, scale 1:50,000. https://doi.org/10.4095/214418.

Bednarski, J. M. (2003h). Surficial geology, Lake Bovie, Northwest Territories – British Columbia. Geological Survey of Canada, Open File 1761, scale 1:50,000. https://doi.org/10.4095/214419.

Bednarski, J. M. (2003i). Surficial geology, Mount Flett, Northwest Territories. Geological Survey of Canada, Open File 4481, scale 1:50,000. https://doi.org/10.4095/214617.

Bednarski, J. M. (2003j). Surficial geology, Muskeg River, Northwest Territories. Geological Survey of Canada, Open File 1753, scale 1:50,000. https://doi.org/10.4095/214408.

Bednarski, J. M. (2003k). Surficial geology, Netla River, Northwest Territories. Geological Survey of Canada, Open File 4478, scale 1:50,000. https://doi.org/10.4095/214561.

Bednarski, J. M. (2003l). Surficial geology, Pointe-de-fleche River, Northwest Territories. Geological Survey of Canada, Open File 1773, scale 1:50,000. https://doi.org/10.4095/214763.

Bednarski, J. M. (2003m). Surficial geology, Rabbit Creek, Northwest Territories. Geological Survey of Canada, Open File 4486, scale 1:50,000. https://doi.org/10.4095/214644.

Bednarski, J. M. (2003n). Surficial geology, Sawmill Mountain, Northwest Territories. Geological Survey of Canada, Open File 4476, scale 1:50,000. https://doi.org/10.4095/214528.

Bednarski, J. M. (2003o). Surficial geology, Tourbiere River, Northwest Territories. Geological Survey of Canada, Open File 4487, scale 1:50,000. https://doi.org/10.4095/214682.

Bednarski, J. M. (2008). Landform assemblages produced by the laurentide Ice sheet in northeastern British Columbia and adjacent Northwest Territories – constraints on glacial lakes and patterns of ice retreat. *Canadian Journal of Earth Sciences*, *45*, 593–610. https://doi.org/10.1139/E07-053

Benn, D., & Evans, D. (2010). *Glaciers and glaciation (2nd ed.)*. Routledge.

Bostock, H. S. (2014). Physiographic regions of Canada. Geological Survey of Canada Map 1254A, scale 1:5,000,000. https://doi.org/10.4095/293408.

Boulton, G. S., & Clark, C. D. (1990a). A highly mobile laurentide Ice sheet revealed by satellite images of glacial lineations. *Nature*, *346*(6287), 813–817. https://doi.org/10.1038/346813a0

Boulton, G. S., & Clark, C. D. (1990b). The laurentide ice sheet through the last glacial cycle. The topology of drift lineations as a key to the dynamic behaviour of former ice sheets. *Transactions of the Royal Society of Edinburgh: Earth Sciences*, *81*(4), 327–347. https://doi.org/10.1017/S0263593300020836

Boulton, G. S., Van Der Meer, J. J. M., Hart, J., Beets, D., Ruegg, G. H. J., Van Der Wateren, F. M., & Jarvis, J.

(1996). Till and moraine emplacement in a deforming bed surge – An example from a marine environment. *Quaternary Science Reviews*, *15*, 961–987. https://doi.org/10.1016/0277-3791(95)00091-7

Brown, V. H. (2012). Ice stream dynamics and pro-glacial lake evolution along the north-west margin of the Laurentide Ice Sheet. PhD thesis. Durham University.

Brown, V. H., Stokes, C. R., & O'Cofaigh, C. (2011). The glacial geomorphology of the north-west sector of the laurentide Ice sheet. *Journal of Maps*, *7*(1), 409–428. https://doi.org/10.4113/jom.2011.1224

Chandler, B. M. P., Lovell, H., Boston, C. M., Lukas, S., Barr, I. D., Benediktsson, ÍÖ, Benn, D. I., Clark, C. D., Darvill, C. M., Evans, D. J. A., Ewertowski, M. W., Loibl, D., Margold, M., Otto, J. C., Roberts, D. H., Stokes, C. R., Storrar, R. D., & Stroeven, A. P. (2018). Glacial geomorphological mapping: A review of approaches and frameworks for best practice. *Earth-Science Reviews*, *185*, 806–846. https://doi.org/10.1016/j.earscirev.2018.07.015

Clark, C. D. (1993). Mega-scale glacial lineations and cross-cutting ice-flow landforms. *Earth Surface Processes and Landforms*, *18*(1), 1–29. https://doi.org/10.1002/esp.3290180102

Clark, C. D. (1999). Glaciodynamic context of subglacial bedform generation and preservation. *Annals of Glaciology*, *28*, 23–32. https://doi.org/10.3189/172756499781821832

Clark, J., Carlson, A. E., Reyes, A. V., Carlson, E. C. B., Guillaume, L., Milne, G. A., Tarasov, L., Caffee, M., Wilcken, K., & Rood, D. H. (2022). The age of the opening of the Ice-free corridor and implications for the peopling of the americas. *PNAS*, *119*(12), e2118558119. https://doi.org/10.1073/pnas.2118558119

Craig, B. G. (1960). *Surficial geology* of north-central district of Mackenzie, Northwest Territories. *Geological Survey of Canada Paper*, 60–18. https://doi.org/10.4095/101204

Craig, B. G. (1965). Glacial lake McConnell and the surficial geology of parts of slave river and redstone river map – areas, district of Mackenzie. *Geological Survey of Canada Bulletin*, *122*), https://doi.org/10.4095/100639

Dalton, A. S., Margold, M., Stokes, C. R., Tarasov, L., Dyke, A. S., Adams, R. S., Allard, S., Arends, H. E., Atkinson, N., Attig, J. W., Barnett, P. J., Barnett, R. L., Batterson, M., Bernatchez, P., Borns, H. W., Breckenridge, A., Briner, J. P., Brouard, E., Campbell, J. E., … Wright, H. T. (2020). An updated radiocarbon-based ice margin chronology for the last deglaciation of the north American Ice sheet complex. *Quaternary Science Reviews*, *234*, 106223. https://doi.org/10.1016/j.quascirev.2020.106223

Duk-Rodkin, A. (1989). Surficial Geology, Norman Wells, Northwest Territories. Geological Survey of Canada, Map 1989A. https://doi.org/10.4095/21361.

Duk-Rodkin, A. (1992). Surficial geology, Fort McPherson-Bell River, Yukon-Northwest Territories. Geological Survey of Canada, Map 1745A, scale 1:250,000. https://doi.org/10.4095/184002.

Duk-Rodkin, A. (2009a). Surficial geology, Wrigley (95O/NW), Northwest Territories. Geological Survey of Canada. Open File 6008, scale 1:100,000. https://doi.org/10.4095/261323.

Duk-Rodkin, A. (2009b). Surficial geology, Wrigley (96O/SW), Northwest Territories. Geological Survey of Canada. Open File 6014, scale 1:100,000. https://doi.org/10.4095/261325.

Duk-Rodkin, A. (2010a). Surficial geology, Kakisa River (85D/SW), Northwest Territories. Geological Survey of Canada. Open File 6012, scale 1:100,000. https://doi.org/10.4095/276737.

Duk-Rodkin, A. (2010b). Surficial geology, Kakisa River (85D/NW), Northwest Territories. Geological Survey of Canada. Open File 6013, scale 1:100,000. https://doi.org/10.4095/282435.

Duk-Rodkin, A. (2011a). Surficial geology, Fort Simpson (95H/NE), Northwest Territories. Geological Survey of Canada, Open File 6010, scale 1:100,000. https://doi.org/10.4095/288767.

Duk-Rodkin, A. (2011b). Surficial geology, Fort Simpson (95H/SE), Northwest Territories. Geological Survey of Canada, Open File 6015, scale 1:100,000. https://doi.org/10.4095/288769.

Duk-Rodkin, A. (2011c). Surficial geology, Fort Simpson (95H/SW), Northwest Territories. Geological Survey of Canada, Open File 6009, scale 1:100,000. https://doi.org/10.4095/288766.

Duk-Rodkin, A. (2011d). Surficial geology, Fort Simpson (95H/NW), Northwest Territories. Geological Survey of Canada, Open File 6011, scale 1:100,000. https://doi.org/10.4095/288768.

Duk-Rodkin, A. (2022). Glacial limits, Mackenzie Mountains and foothills, Northwest Territories, Canada. Geological Survey of Canada, Open File 8891, 1:1,000,000 scale. https://doi.org/10.4095/330011.

Duk-Rodkin, A., & Couch, A. (2004). Surficial geology, Fort Norman, Northwest Territories. Geological Survey of Canada, Open File 4662, scale 1:250,000. https://doi.org/10.4095/215648.

Duk-Rodkin, A., & Hughes, I. L. (1992a). Surficial geology, Arctic Red River, District if Mackenzie, Northwest Territories. Geological Survey of Canada, Map 1746A, scale 1:250,000. https://doi.org/10.4095/184003.

Duk-Rodkin, A., & Hughes, I. L. (1992b). Surficial geology, Canot Lake, District of Mackenzie, Northwest Territories. Geological Survey of Canada, Map 1748A, scale 1:250,000. https://doi.org/10.4095/184005.

Duk-Rodkin, A., & Hughes, I. L. (1992c). Surficial geology, Fort Good Hope, District of Mackenzie, Northwest Territories. Geological Survey of Canada. Map 1741A, scale 1:250,000. https://doi.org/10.4095/183998.

Duk-Rodkin, A., & Hughes, I. L. (1992d). Surficial geology, Martin House, Yukon – Northwest Territories. Geological Survey of Canada, Map 1743A, scale 1:250,000. https://doi.org/10.4095/184000.

Duk-Rodkin, A., & Hughes, I. L. (1992e). Surficial geology, Ontaratue River, District of Mackenzie, Northwest Territories. Geological Survey of Canada, Map 1742A, scale 1:250,000. https://doi.org/10.4095/183999.

Duk-Rodkin, A., & Hughes, I. L. (1992f). Surficial geology, Travaillant Lake, District of Mackenzie, Northwest Territories. Geological Survey of Canada, Map 1747A, scale 1:250,000. https://doi.org/10.4095/184004.

Duk-Rodkin, A., & Hughes, I. L. (1993a). Surficial geology, Sans Sault Rapids, District of Mackenzie, Northwest Territories. Geological Survey of Canada, Map 1784A, scale 1:250,000. https://doi.org/10.4095/184008.

Duk-Rodkin, A., & Hughes, I. L. (1993b). Surficial geology, Upper Ramparts River, District of Mackenzie, Northwest Territories. Geological Survey of Canada, Map 1783A, scale 1:250,000. https://doi.org/10.4095/184153.

Duk-Rodkin, A., & Huntley, D. (2018). Surficial geology, Root River, Northwest Territories, NTS 95-K northeast. Geological Survey of Canada, Canadian Geoscience Map 295, scale 1:100,000. https://doi.org/10.4095/299111.

Dulfer, H. E., & Margold, M. (2021). Glacial geomorphology of the central sector of the cordilleran Ice sheet, northern British Columbia, Canada. *Journal of Maps*, *17*(2), 413–427. https://doi.org/10.1080/17445647.2021.1937729

Dulfer, H. E., Margold, M., Darvill, C. M., & Stroeven, A. P. (2022). Reconstructing the advance and retreat dynamics of the central sector of the last cordilleran Ice sheet. *Quaternary Science Reviews*, *284*, 107465. https://doi.org/10.1016/j.quascirev.2022.107465

Dunlop, P., & Clark, C. D. (2006). The morphological characteristics of ribbed moraine. *Quaternary Science Reviews*, *25*(13-14), 1668–1691. https://doi.org/10.1016/j.quascirev.2006.01.002

Dyke, A. S. (2004). *An outline of north American deglaciation with emphasis on central and northern Canada*. In J. Ehlers, & P. L. Gibbard (Eds.), *Quaternary glaciations – extent and chronology, part II* (pp. 373–424). Elsevier. https://doi.org/10.1016/S1571-0866(04)80209-4.

Dyke, A. S., & Morris, T. F. (1988). Canadian landform examples. Drumlin fields, dispersal trains, and ice streams in Arctic Canada. *The Canadian Geographer*, *32*(1), 86–90. https://doi.org/10.1111/j.1541-0064.1988.tb00860.x

Ednie, M., Kerr, D. E., Olthof, I., Wolfe, S. A., & Eagles, S. (2014). Predictive surficial geology derived from LANDSAT 7, Marian River, NTS 85-N, Northwest Territories. Geological Survey of Canada, open file 7543, scale 1:125,000. https://doi.org/10.4095/294923.

Ely, J. C., Clark, C. D., Spagnolo, M., Stokes, C. R., Greenwood, S. L., Hughes, A. L. C., Dunlop, P., & Hess, D. (2016). Do subglacial bedforms comprise a size and shape continuum? *Geomorphology*, *257*, 108–119. https://doi.org/10.1016/j.geomorph.2016.01.001

EROS, United States Geological Survey's Center for Earth Resources Observation and Science. (2010). 30 arc-second DEM of North America. Available at https://databasin.org/datasets/d2198be9d2264de19cb93fe6a380b69c/. Accessed on 1 April 2021

Evans, D. J. A., Smith, I. R., Gosse, J. C., & Galloway, J. M. (2021). Glacial landforms and sediments (landsystem) of the smoking hills area, Northwest Territories, Canada: Implications for regional pliocene-pleistocene laurentide Ice sheet dynamics. *Quaternary Science Reviews*, *262*, 106958. https://doi.org/10.1016/j.quascirev.2021.106958

Evans, D. J. A., Storrar, R. D., & Rea, B. R. (2016). Crevasse-squeezed ridge corridors: Diagnostic features of late-stage paleo-ice stream activity. *Geomorphology*, *258*, 40–50. https://doi.org/10.1016/j.geomorph.2016.01.017

Geological Survey of Canada. (2014a). Surficial geology, Contwoyto Lake, Northwest Territories – Nunavut, NTS 76-E. Geological Survey of Canada, Canadian Geoscience Map 198, scale 1:125,000. https://doi.org/10.4095/295192

Geological Survey of Canada. (2014b). Surficial geology, Inman River, Nunavut, NTS 87-B and parts of NTS 87-A, NTS 87-C, and NTS 87-D. Geological Survey of Canada, Canadian Geoscience Map 185, scale 1:250,000. https://doi.org/10.4095/295498.

Geological Survey of Canada. (2014c). Surficial geology, Lac de Gras, Northwest Territories, NTS 76-D. Geological Survey of Canada, Canadian Geoscience Map 184, scale 1:125,000. https://doi.org/10.4095/295497.

Geological Survey of Canada. (2015). Surficial geology, Winter Lake, Northwest Territories, NTS 86-A. Geological Survey of Canada, Canadian Geoscience Map 196, scale 1:125,000. https://doi.org/10.4095/295588

Geological Survey of Canada. (2016a). Surficial geology, Buffalo Lake, Northwest Territories, NTS 85-B. Geological Survey of Canada, Canadian Geoscience Map 2002, scale 1:250,000. https://doi.org/10.4095/298705.

Geological Survey of Canada. (2016b). Surficial geology, Klewi River, Northwest Territories, NTS 85-A. Geological Survey of Canada, Canadian Geoscience Map 219, scale 1:250,000. https://doi.org/10.4095/298704

Geological Survey of Canada. (2016c). Surficial geology, Napaktulik Lake, Nunavut, NTS 86-I. Geological Survey of Canada, Canadian Geoscience Map 235, scale 1:125,000. https://doi.org/10.4095/298708

Geological Survey of Canada. (2016d). Surficial geology, Point Lake, Northwest Territories – Nunavut, NTS 86-H. Geological Survey of Canada, Canadian Geoscience Map 218, scale 1:125,000. https://doi.org/10.4095/298703

Geological Survey of Canada. (2017a). Surficial geology, Carcajou Canyon, Northwest Territories, NTS 96-D. Geological Survey of Canada, Canadian Geoscience Map 335, scale 1:250,000. https://doi.org/10.4095/306167.

Geological Survey of Canada. (2017b). Surficial geology, Hepburn Island, Nunavut, NTS 79-M. Geological Survey of Canada, Canadian Geoscience Map 228, scale 1:125,000. https://doi.org/10.4095/299205.

Geological Survey of Canada. (2017c). Surficial geology, Kikerk Lake, Northwest Territories, NTS 86-P. Geological Survey of Canada, Canadian Geoscience Map 229, scale 1:125,000. https://doi.org/10.4095/299206.

Geological Survey of Canada. (2018a). Reconnaissance surficial geology, Sibbeston Lake, Northwest Territories, NTS 95-G. Geological Survey of Canada, Canadian Geoscience Map 364, scale 1:125,000. https://doi.org/10.4095/308365.

Geological Survey of Canada. (2018b). Surficial geology, Fort Simpson, Northwest Territories, NTS 95-H. Geological Survey of Canada, Canadian Geoscience Map 369, scale 1:125,000. https://doi.org/10.4095/308384.

Geological Survey of Canada. (2019a). Reconnaissance surficial geology, Bulmer Lake, Northwest Territories, NTS 95-I. Geological Survey of Canada, Canadian Geoscience Mao 365, scale 1:125,000. https://doi.org/10.4095/308378.

Geological Survey of Canada. (2019b). Reconnaissance surficial geology, Camsell Bend, Northwest Territories, NTS 95-J. Geological Survey of Canada, Canadian Geoscience Map 370, scale 1:125,000. https://doi.org/10.4095/308483.

Geological Survey of Canada. (2019c). Reconnaissance surficial geology, Wrigley Lake, Northwest Territories, NTS 95-O. Geological Survey of Canada, Canadian Geoscience Map 371, scale 1:125,000. https://doi.org/10.4095/308491

Geological Survey of Canada, (2019d). Surficial geology, Dahadinni River, Northwest Territories, NTS 95-N northwest. Geological Survey of Canada, Canadian Geoscience Map 298. Scale 1:125,000. https://doi.org/10.4095/299113

Geological Survey of Canada. (2022a). Reconnaissance surficial geology, Blackwater Lake, Northwest Territories, NTS 96-B. Geological Survey of Canada, Canadian Geoscience Map 386. Scale 1:250,000. https://doi.org/10.4095/313108

Geological Survey of Canada. (2022b). Reconnaissance surficial geology, Sambaa K'e, Northwest Territories, NTS 95-A. Geological Survey of Canada, Canadian Geoscience Map 374. Scale 1:250,000. https://doi.org/10.4095/311228

Geological Survey of Canada. (2022c). Surficial geology, Kakisa River, Northwest Territories, NTS 85-D.

Geological Survey of Canada, Canadian Geoscience Map 372. Scale 1:125,000. https://doi.org/10.4095/308493.

Government of Canada. (2013). Landsat Image Mosaic of Canada. Natural Resources Canada, Canadian Forest Service, Pacific Forestry Centre. Available at https://ftp.maps.canada.ca/pub/nrcan_rncan/archive/image/landsat_7/canada_mosaic/. Accessed 1 April 2021

Greenwood, S. L., Clark, C. D., & Hughes, A. L. C. (2007). Formalising an inversion methodology for reconstructing ice-sheet retreat patterns from meltwater channels: Application to the British Ice sheet. *Journal of Quaternary Science*, *22*(6), 637–645. https://doi.org/10.1002/jqs.1083

Greenwood, S. L., Clason, C. C., Helanow, C., & Margold, M. (2016). Theoretical, contemporary observational and palaeo-perspectives on ice sheet hydrology: Processes and products. *Earth-Science Reviews*, *155*, 1–27. https://doi.org/10.1016/j.earscirev.2016.01.010

Hagedorn, G. W., Smith, I. R., Paulen, R. C., & Ross, M. (2022). Surficial geology, Enterprise, Northwest Territories, NTS 85-C/9, 10, 15 and 16. Geological Survey of Canada, Canadian Geoscience Mao 438, scale 1:100,000. https://doi.org/10.4095/328292.

Hättestrand, C., & Kleman, J. (1999). Ribbed moraine formation. *Quaternary Science Reviews*, *18*(1), 43–61. https://doi.org/10.1016/S0277-3791(97)00094-2

Hebrand, M., & Åmark, M. (1989). Esker formation and glacier dynamics in eastern skane and adjacent areas, southern Sweden. *Boreas*, *18*(1), 67–81. https://doi.org/10.1111/j.1502-3885.1989.tb00372.x

Huntley, D., Mills, A., & Paulen, R. (2008). Surficial deposits, landforms, glacial history and reconnaissance drift sampling in the Trout Lake map area, Northwest Territories. Geological Survey of Canada, Current Research (online) no. 2008-14. https://doi.org/10.4095/225636.

Kennedy, K. E., Froese, D. G., Zazula, G. D., & Lauriol, B. (2010). Last glacial maximum age of the northwest laurentide maximum from the eagle river spillway and delta complex, northern Yukon. *Quaternary Science Reviews*, *29*(9-10), 1288–1300.

Kerr, D. E. (2014). Reconnaissance surficial geology, MacKay Lake, Northwest Territories, NTS 75-M. Geological Survey of Canada, Canadian Geoscience Map 206 (preliminary), scale 1:125,000. https://doi.org/10.4095/295542.

Kerr, D. E. (2018). Reconnaissance surficial geology, Kathawachaga Lake, Nunavut, NTS 76-L. Geological Survey of Canada, Canadian Geoscience Map 363, scale 1:125,000. https://doi.org/10.4095/308367.

Kerr, D. E. (2022a). Reconnaissance surficial geology, Bebensee Lake, Northwest Territories-Nunavut, NTS 86-M. Geological Survey of Canada, Canadian Geoscience Map 451, scale 1:125,000. https://doi.org/10.4095/329456.

Kerr, D. E. (2022b). Reconnaissance surficial geology, Bloody River, Northwest Territories-Nunavut, NTS 96-P. Geological Survey of Canada, Canadian Geoscience Map 452, scale 1:125,000. https://doi.org/10.4095/329457.

Kerr, D. E. (2022c). Reconnaissance surficial geology, Cape MacDonnel, Northwest Territories, NTS 96-I. Geological Survey of Canada, Canadian Geoscience Map 453, scale 1:125,000. https://doi.org/10.4095/330074.

Kerr, D. E. (2022d). Reconnaissance surficial geology, Keller Lake, Northwest Territories, NTS 95-P. Geological Survey of Canada, Canadian Geoscience Map 439, scale 1:125,000. https://doi.org/10.4095/328293.

Kerr, D.E. (2022e). Reconnaissance surficial geology, Sloan River, Northwest Territories-Nunavut, NTS 86-K. Geological Survey of Canada, Canadian Geoscience Map 450, scale 1:125,000. https://doi.org/10.4095/329452.

Kerr, D. E., Knight, R. D., Sharpe, D. R., Cummings, D. I., & Kjarsgaard, B. A. (2014). Surficial Geology, Snowdrift, Northwest Territories, NTS 75-L. Geological Survey of Canada, Canadian Geoscience Map 137 (2nd edition, preliminary), scale 1:125,000. https://doi.org/10.4095/295496.

Kerr, D. E., Morse, P. D., & Wolfe, S. A. (2016). Reconnaissance surficial geology, Rae, Northwest Territories, NTS 85-K. Geological Survey of Canada, Canadian Geoscience Map 290 (preliminary), scale 1:125,000. https://doi.org/10.4095/298838.

Kerr, D. E., Morse, P. D., & Wolfe, S.A. (2017a). Reconnaissance surficial geology, Lac la Matre, Northwest Territories, NTS 85-M. Geological Survey of Canada, Canadian Geoscience Map 306, scale 1:125,000. https://doi.org/10.4095/304282.

Kerr, D. E., Morse, P. D., & Wolfe, S. A. (2017b). Reconnaissance surficial geology, Willow Lake, Northwest Territories, NTS 85-L. Geological Survey of Canada, Canadian Geoscience Map 304 (preliminary), scale 1:125,000. https://doi.org/10.4095/299468.

Kerr, D. E., & O'Neil, H. B., (2017). Reconnaissance surficial geology, Indin Lake, Northwest Territories, NTS 86-B. Geological Survey of Canada, Canadian Geoscience Map 334 (preliminary), scale 1:125,000. https://doi.org/10.4095/306108.

Kerr, D. E., & O'Neil, H. B. (2018a). Reconnaissance surficial geology, Hardisty Lake, Northwest Territories, NTS 86-C. Geological Survey of Canada, Canadian Geoscience Map 337 (preliminary), scale 1:125,000. https://doi.org/10.4095/306290.

Kerr, D. E., & O'Neil, H. B. (2018b). Reconnaissance surficial geology, Rivière Grandin, Northwest Territories, NTS 86-D. Geological Survey of Canada, Canadian Geoscience Map 361, scale 1:125,000. https://doi.org/10.4095/308479.

Kerr, D. E., & O'Neil, H. B. (2019a). Reconnaissance surficial geology, Calder River, Northwest Territories, NTS 86-F. Geological Survey of Canada, Canadian Geoscience Mao 389, scale 1:125,000. https://doi.org/10.4095/313519.

Kerr, D. E., & O'Neil, H. B. (2019b). Reconnaissance surficial geology, Leith Peninsula, Northwest Territories, NTS 86-E. Geological Survey of Canada, Canadian Geoscience Mao 409, scale 1:125,000. https://doi.org/10.4095/314705.

Kerr, D. E., & O'Neil, H. B. (2019c). Reconnaissance surficial geology, Takaatcho River, Northwest Territories, NTS 86-L. Geological Survey of Canada, Canadian Geoscience Map 388, scale 1:125,000. https://doi.org/10.4095/313282.

Kerr, D. E., & O'Neil, H. B. (2020). Reconnaissance surficial geology, Johnny Hoe River, Northwest Territories, NTS 96-A. Geological Survey of Canada, Canadian Geoscience Map 424, scale 1:125,000. https://doi.org/10.4095/321631.

Kerr, D. E., & O'Neil, H. B. (2021). Reconnaissance surficial geology, Grizzly Bear Mountain, Northwest Territories, NTS 96-H. Geological Survey of Canada, Canadian Map 425, scale 1:250,000. https://doi.org/10.4095/321745.

King, E. C., Hindmarsh, R. C., & Stokes, C. R. (2009). Formation of mega-scale glacial lineations observed beneath the west antarctic Ice stream. *Nature Geoscience*, *2*(8), 585–588. https://doi.org/10.1038/ngeo581

Klassen, R. W. (1971). Surficial geology, Franklin Bay and Brock River, District of Mackenzie, Northwest Territories. Geological Survey of Canada Open File 48. https://doi.org/10.4095/129145.

Kleman, J., & Borgström, I. (1996). Reconstruction of paleo-ice sheets: The use of geomorphological data. *Earth Surface Processes and Landforms*, *21*(10), 893–909. https://doi.org/10.1002/(SICI)1096-9837(199610)21:10<893::AID-ESP620>3.0.CO;2-U

Kleman, J., & Glasser, N. F. (2007). The subglacial thermal organization (STO) of ice sheets. *Quaternary Science Reviews*, *26*(5-6), 585–597. https://doi.org/10.1016/j.quascirev.2006.12.010

Kleman, J., Hättestrand, C., Borgström, I., & Stroeven, A. (1997). Fennoscandian palaeoglaciology reconstructed using a glacial geological inversion model. *Journal of Glaciology*, *43*(144), 283–299. https://doi.org/10.3189/S0022143000003233

Kleman, J., Hättestrand, C., Stroeven, A. P., Jansson, K. N., De Angelis, H., & Borgström, I. (2006). Reconstruction of palaeo-ice sheets – inversion of their glacial geomorphological record. In P. G. Knight (Ed.), *Glacier science and environmental change*. Blackwell Publishing Ltd. https://doi.org/10.1002/9780470750636.ch38.

Kleman, J., Jansson, K., De Angelis, H., Stroeven, A. P., Hättestrand, C., Alm, G., & Glasser, N. (2010). North American Ice sheet build-up during the last glacial cycle, 115–21 kyr. *Quaternary Science Reviews*, *29*(17–18), 2036–2051. https://doi.org/10.1016/j.quascirev.2010.04.021

Koster, E. A. (1988). Ancient and modern cold-climate aeolian sand deposition: A review. *Journal of Quaternary Science*, *3*(1), 69–83. https://doi.org/10.1002/jqs.3390030109

Lemmen, D. S., Duk-Rodkin, A., & Bednarski, J. M. (1994). Late glacial drainage systems along the northwestern margin of the laurentide Ice sheet. *Quaternary Science Reviews*, *13*, 805–828. https://doi.org/10.1016/0277-3791(94)90003-5

Lindholm, M. S., & Heyman, J. (2016). Glacial geomorphology of the maidika region, Tibetan plateau. *Journal of Maps*, *12*(5), 797–803. https://doi.org/10.1080/17445647.2015.1078182

Lundqvist, J. (1989). Rogen (ribbed) moraine – identification and possible origin. *Sedimentary Geology*, *62*(2–4), 281–292. https://doi.org/10.1016/0037-0738(89)90119-X

Mannerfelt, J. M. (1949). Marginal drainage channels as indicators of the gradients of quaternary ice caps. *Geografiska Annaler*, *31*, 194–199.

Margold, M., Jansson, K. N., Kleman, J., & Stroeven, A. P. (2011). Glacial meltwater landforms of central British Columbia. *Journal of Maps*, *7*(1), 486–506. https://doi.org/10.4113/jom.2011.1205

Margold, M., Stokes, C. R., & Clark, C. D. (2015a). Ice streams in the laurentide Ice sheet: Identification, characteristics and comparison to modern ice sheets. *Earth-Science Reviews*, *143*, 117–146. https://doi.org/10.1016/j.earscirev.2015.01.011

Margold, M., Stokes, C. R., & Clark, C. D. (2018). Reconciling records of ice streaming and ice margin retreat to produce a palaeogeographic reconstruction of the deglaciation of the laurentide Ice sheet. *Quaternary Science Reviews*, *189*, 1–30. https://doi.org/10.1016/j.quascirev.2018.03.013

Margold, M., Stokes, C. R., Clark, C. D., & Kleman, J. (2015b). Ice streams of the laurentide Ice sheet: A new mapping inventory. *Journal of Maps*, *11*, 380–395. https://doi.org/10.1080/17445647.2014.912036

Morse, P.D., Kerr, D.E., Wolfe, S.A., & Olthof, I. (2016). Predictive surficial geology, Wecho River, Northwest Territories, NTS 85-O. Geological Survey of Canada, Geoscience Map 227, scale 1:125,000. https://doi.org/10.4095/298686.

Natural Resources Canada. (2012). North Canada. The Atlas of Canada Reference Map Series. Scale 1:4,000,000.

Norris, S. L., Margold, M., & Froese, D. G. (2017). Glacial landforms of northwest Saskatchewan. *Journal of Maps*, *13*(2), 600–607. https://doi.org/10.1080/17445647.2017.1342212

Olthof, I., Kerr, E. E., Wolfe, S. A., & Eagles, S. (2014). Predictive surficial materials and surficial geology from LANDSAT-7, Upper Carp Lake, NTS 85-P, Northwest Territories. Geological Survey of Canada, Open file 7601. https://doi.org/10.4095/293970.

Paulen, R.C., & Smith, I.R. (2022). Surficial geology, Sulphur Bay, Western Great Slave Lake, Northwest Territories, NTS 85-G. Geological Survey of Canada, Canadian Geoscience Map 443, scale:125,000. https://doi.org/10.4095/330073.

Porter, C., Morin, P., Howat, I., Noh, M. J., Bates, B., Peterman, K., Keesey, S., Schlenk, M., Gardiner, J., Tomko, K., Willis, M., Kelleher, C., Cloutier, M., Husby, E., Foga, S., Nakamura, H., Platson, M., Wethington, M., Williamson, C., … Bojesen, M. (2018). ArcticDEM. Available at https://doi.org/10.7910/DVN/OHHUKH. Harvard Dataverse, V1. Accessed on 1 April 2021

Prest, V.K., Grant, D.R., & Rampton, V.N. (1968). Glacial map of Canada. Geological Survey of Canada, "A" Series Map 1253A. https://doi.org/10.4095/108979.

Rampton, V. N. (1988). *Quaternary geology of the tuktoyaktuk coastlands, Northwest Territories*. Geological survey of Canada. *Memoir*, *423*), https://doi.org/10.4095/126937

Reyes, A. V., Carlson, A. E., Milne, G. A., Tarasov, L., Reimink, J. R., & Caffee, M. W. (2022). Revised chronology of the northwest laurentide ice-sheet deglaciation from ^{10}Be exposure ages on boulder erratics. *Quaternary Science Reviews*, *277*, 107369. https://doi.org/10.1016/j.quascirev.2021.107369

Rutter, N. W., Hawes, R. J., & Catto, N. R. (1993). Surficial geology, Southern Mackenzie River Valley, District of Mackenzie, Northwest Territories. Geological Survey of Canada, Map 1693A, scale 1:500,000. https://doi.org/10.4095/193343.

Rutter, N. W., Minning, G. V., & Netterville, J. A. (1980). Surficial geology and geomorphology, Mills Lake, District of Mackenzie. Geological Survey of Canada, Preliminary Map 15-1978. https://doi.org/10.4095/109708.

Shaw, J., Sharpe, D., & Harris, J. (2010). A flowline map of glaciated Canada based on remote sensing data. *Canadian Journal of Earth Sciences*, *47*(1), 89–101. https://doi.org/10.1139/E09-068

Shreve, R. L. (1985). Esker characteristics in terms of glacier physics, katahdin esker system, Maine. *Geological Society of America Bulletin*, *96*(5), 639–646. https://doi.org/10.1130/0016-7606(1985)96<639:ECITOG>2.0.CO;2

Slaymaker, O., & Kovanen, D. J. (2017). Long-term geomorphic history of western Canada. In O. Slaymaker (Ed.), *Landscapes and landforms of western Canada*. Springer International Publishing Switzerland. https://doi.org/10.1007/978-3-319-44595-3.

Smith, I. R., Paulen, R. C., & Hagedorn, G. W. (2021). Surficial geology, Northeastern Cameron Hills, Northwest Territories, NTS 85-C/3, 4, 5 and 6. Geological Survey of Canada, Canadian Geoscience Map 431, scale 1:100,000. https://doi.org/10.4095/328129.

Spagnolo, M., Clark, C. D., Ely, J. C., Stokes, C. R., Anderson, J. B., Andreassen, K., Graham, A. G. C., & King, E. C. (2014). Size, shape and spatial arrangement of mega-scale glacial lineations from a large and diverse dataset. *Earth Surface Processes and Landforms*, *39*(11), 1432–1448. https://doi.org/10.1002/esp.3532

Stevens, C. W., Kerr, D. E., Wolfe, S. A., & Eagles, S. (2017). Predictive surficial geology, Yellowknife and Hearne Lake, Northwest Territories, NTS 85-J and 85-I. Geological Survey of Canada, Canadian Geoscience Map 200 (2nd edition, preliminary), scale 1:125,000. https://doi.org/10.4095/299516.

Stoker, B. J., Margold, M., Gosse, J. C., Hidy, A. J., Monteath, A. J., Young, J. M., Gandy, N., Gregoire, L., Norris, S. L., & Froese, D. (2022). The collapse of the laurentide-cordilleran ice saddle and early opening of the Mackenzie valley, Northwest Territories, constrained by ^{10}Be exposure dating. *The Cryosphere*, *16*, 4865–4886. https://doi.org/10.5194/tc-2022-120

Stokes, C. R., & Clark, C. D. (1999). Geomorphological criteria for identifying pleistocene ice streams. *Annals of Glaciology*, *28*, 67–74. https://doi.org/10.3189/172756499781821625

Stokes, C. R., & Clark, C. D. (2002). Ice stream shear margin moraine. *Earth Surface Processes and Landforms*, *27*, 547–588. https://doi.org/10.1002/esp.326

Stokes, C. R., Margold, M., & Creyts, T. (2016). Ribbed bedforms on palaeo-ice stream beds resemble regular patterns of basal shear stress ('traction ribs') inferred from modern ice streams. *Journal of Glaciology*, *62*(234), 696–713. https://doi.org/10.1017/jog.2016.63

Stokes, C. R., Tarasov, L., Blomdin, R., Cronin, T. M., Fisher, T. G., Gyllencreutz, R., Hättestrand, C., Heyman, J., Hindmarsh, R. C., Hughes, … Teller, J. T. (2015). On the reconstruction of palaeo-ice sheets: Recent advances and future challenges. *Quaternary Science Reviews*, *125*, 15–49. https://doi.org/10.1016/j.quascirev.2015.07.016

St-Onge, D. A. (1988). Surficial geology of Coppermine River, District of Mackenzie, Northwest Territories. Geological Survey of Canada, A Series Map 1645A. https://doi.org/10.4095/126431.

Storrar, R. D., Ewertowski, M., Tomczyk, A. M., Barr, I. D., Livingstone, S. J., Ruffell, A., Stoker, B. J., & Evans, D. J. A. (2020). Equifinality and preservation potential of complex eskers. *Boreas*, *49*(1), 211–231. https://doi.org/10.1111/bor.12414

Storrar, R. D., Stokes, C. R., & Evans, D. J. A. (2014). Morphometry and pattern of a large sample (>20,000) of Canadian eskers and implications for subglacial drainage beneath ice sheets. *Quaternary Science Reviews*, *105*, 1–25. https://doi.org/10.1016/j.quascirev.2014.09.013

Stroeven, A. P., Hättestramd, C., Heyman, J., Kleman, J., & Morén, B. M. (2013). Glacial geomorphology of the Tian Shan. *Journal of Maps*, *9*(4), 505–512. https://doi.org/10.1080/17445647.2013.820879

Stroeven, A. P., Hättestrand, C., Kleman, J., Heyman, J., Febel, D., Fredin, O., Goodfellow, B. W., Harbor, J. M., Jansen, J. D., Olsen, L., Caffee, M. W., Fink, D., Lundqvist, J., Rosqvist, G. C., Strömberg, B., & Jansson, K. N. (2016). Deglaciation of fennoscandia. *Quaternary Science Reviews*, *147*, 91–121. https://doi.org/10.1016/j.quascirev.2015.09.016

Veillette, J. J., St-Onge, D. A., & Kerr, D.E. (2013a). Surficial geology, Brock River, Northwest Territories – Nunavut, NTS 97-D. Geological Survey of Canada, Canadian Geoscience Map 112 (preliminary), scale 1:250,000. https://doi.org/10.4095/292246.

Veillette, J. J., St-Onge, D. A., & Kerr, D.E. (2013b). Surficial geology, Erly Lake, Northwest Territories – Nunavut, NTS 97-A. Geological Survey of Canada, Canadian Geoscience Map 111 (preliminary), scale 1:250,000. https://doi.org/10.4095/292245.

Wolfe, S. A., Huntley, D. J., & Ollerhead, J. (2004). Relict late wisconsinan dune fields of the northern great plains. *Canada. Géographie Physique et Quaternaire*, *28*(2-3), 323–336. https://doi.org/10.7202/013146ar